

MODELING AND SIMULATION OF AN INDUSTRIAL INDIRECT SOLAR DRYER FOR IROKO WOOD (*Chlorophora excelsa*) IN A TROPICAL ENVIRONMENT

Merlin Simo-Tagne^{1,*}, André Zoulalian², Romain Remond³, Yann Rogaume³,
Beguidé Bonoma⁴

ABSTRACT

This paper presents a modeling of an instrumental indirect solar wood dryer less expensive functioning in a Cameroonian climate applied to the climate of Yaoundé. The dryer is easy to build and electric energy is only used for the fan. Applications are done on Iroko wood (*Chlorophora excelsa*), a tropical wood 50mm thick most utilized in Africa. A satisfactory agreement between experimental and numerical results was found. Influences of thickness, wood initial water content and airflow rate were studied.

Keywords: Drying curves, numerical simulation, solar greenhouse dryer, tropical climate, tropical woods.

INTRODUCTION

In Cameroon, forest exploitation gives provides considerable to the state. In addition, natural forests represent an important area. Iroko (*Chlorophora excelsa*) is prohibited exporting in the form of rough lumber. Then, it is very important to develop the first transformations in the country. For this reason, the reflections to optimize the drying are necessary in function of the local realities. Locally, after sawing, natural drying is used in the majority to dry wood. This method is known to have a lot of drying time and to destroy more boards than solar drying in an appropriate dryer. Solar drying is a method recommended where sustainable development is essential to reduce the environment impact of the industrial activities.

Cameroon has good solar potential with an average incident solar energy from 4,5 kWh/m² in the south and 5,8kWh/m² daily in the great north (Ayangma *et al.* 2008). For example, the study of Ayangma *et al.* (2008) using 20 years data and applied in Garoua, a city of the great north region of

¹LERMaB, Post-Doctoral position, 27 rue Philippe Séguin, P.O. Box 1041, F-88051 Epinal, France.

²University of Lorraine, LERMaB, Faculty of Sciences and Technologies, Aiguillettes Campus, P.O. Box 70239-54506 VIN, Nancy, France.

³University of Lorraine, LERMaB, ENSTIB, 27 rue Philippe Séguin, P.O. Box 1041, F-88051 Epinal, France.

⁴Higher Teacher's Training College, Applied Physic Laboratory, P.O.Box 47, Yaoundé, Cameroon.

*Corresponding author: simotagne2002@yahoo.fr

Received: 17.01.2016 Accepted: 20.11.2016

Cameroon gives an estimation near 5,743 kWh/(m².day). Another works in the literature such as Lealea and Tchinda (2013) and Njomo and Wald (2006) present some estimations of solar irradiation of many Cameroonian towns in general. Figure 1 presents the position of Cameroon's incident solar energy with some others developing countries.

In the literature, we have solar dryers with the wall in glass or with energy storage (Awadalla *et al.* 2004, Bauer 2003, Bekkioui 2009, Bekkioui *et al.* 2009, Bekkioui *et al.* 2011, Bentayeb *et al.* 2008a, Bentayeb *et al.* 2008b, Luna 2008, Luna *et al.* 2010). These dryers are very expensive for the level of development of many people coming in tropical region. Mathematical modeling is an essential tool that facilitates the understanding of the physical phenomena occurring in the product to dry during solar drying. It is possible to numerically model a dryer in order to give the characteristics to impose during the construction and to satisfy the needs of a population.

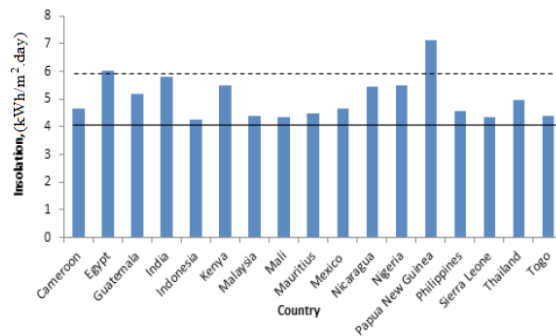


Figure 1. Global solar irradiation on a horizontal plane of some developing countries (Weiss and Buchinger 2003)

In this work, a modeling and a numerical simulation of the instrumental solar dryer of tropical woods coming from Cameroon are done. The price of construction of this simple dryer is low. The environment of the drying is the one of Yaoundé. Experiments are done from 22th November to 12th December 2004. Before, we present a model for the desorption isotherms based on experimental values presented in the literature.

MATERIAL AND METHODS

Modeling of the desorption isotherms

We have used experimental values (Jannot *et al.* 2006) to propose a relation for the isotherms of desorption. For the equilibrium moisture content (X_{eq} , -) as a function of temperature (T , K) and fractional relative humidity (HR , -), we obtained:

$$X_{eq} = \frac{b_1 X_m HR}{(1 - b_2 HR)(1 - b_2 HR + b_1 HR)} \quad (1a)$$

$$X_m = -7,33 \times 10^{-4} T + 0,286; \quad R^2 = 0,994 \quad (1b)$$

$$b_2 = 1,931 \exp\left(\frac{-2308,798}{RT}\right); \quad R^2=0,919 \tag{1c}$$

$$b_1 = 27,827 \exp\left(\frac{-2135,87}{RT}\right); \quad R^2=0,324 \tag{1d}$$

Figure 2a illustrates the equilibrium moisture content of the desorption summarized in Eq (1a).

The fractional moisture content at the fiber saturation point (X_{fsp} -) is obtained using Eq (1a) with a value of 1 for relative humidity. This is presented in Eq (2) and plotted as a function of temperature in Figure 2b.

$$X_{fsp} = \frac{b_1 X_m}{(1-b_2)(1-b_2+b_1)} \tag{2}$$

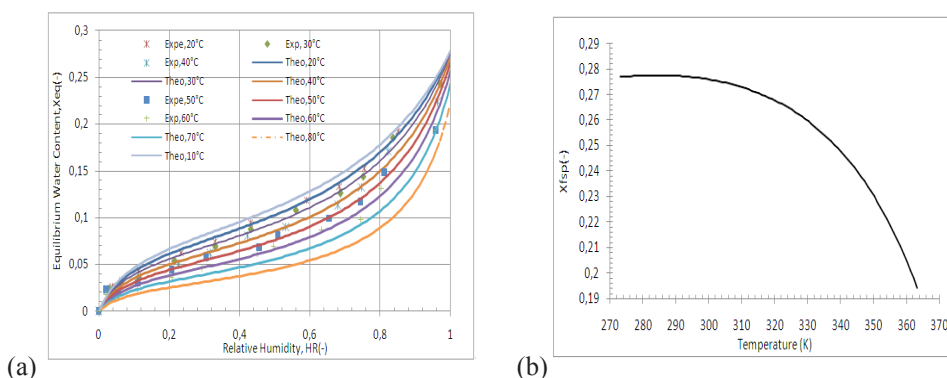


Figure 2. (a) Experimental and theoretical (Dent’s model) isotherms of desorption of Iroko wood and (b) evolution of the fiber saturation point versus temperature.

Solar data

The drying was done in Yaoundé. After using the data given in Kemajou *et al.* (2012), we obtained Equations (3a) and (3b) of the correlations of experimental values of diffuse and global insulation on a horizontal plane in Yaoundé respectively. Geographical coordinates of Yaoundé are: Latitude: 3,87°N; Longitude: 11,52°E; Altitude: 720m (Afungchui and Neba-Ngwa 2013).

$$D=0,12152t^4-5,44546t^3+76,93216t^2-349,09338t+357,73432 ; R^2=0,99967 \tag{3a}$$

$$G_t=0,51681t^4-24,19623t^3+386,86802t^2-2427,06266t+5207,34134 ; R^2=0,99882 \tag{3b}$$

Using the relationships given in Appendix A, we have deduced the global irradiations on a slope plane at 10° (3c) and on the wall at 90° (3d).

$$G_t^*(10^\circ) = -0,02411t^5 + 1,86434t^4 - 53,12658t^3 + 685,0667t^2 - 3906,6173t + 8037,91894; R^2 = 0,99 \quad (3c)$$

$$G_t^*(\text{Wall}) = 0,12073t^4 - 5,32896t^3 + 74,29878t^2 - 332,08327t + 312,788 \quad ; R^2 = 0,9913 \quad (3d)$$

Where t is the time of the day in hour. Between 6am and 6pm, G_t^* is given by (3c) and (3d) on the slope and the wall respectively. At night, G_t^* is equal to zero. Figure 3 presents the diffuse and global solar irradiation on horizontal plane experimentally obtained by Kemajou *et al.* (2012) and estimations of these physical parameters on inclined plane with 10° angle.

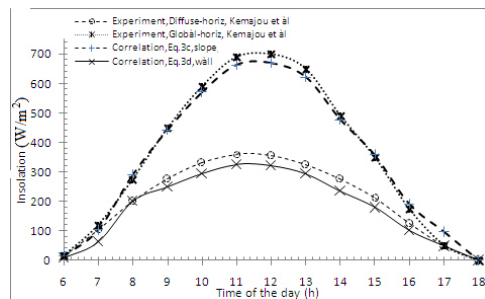


Figure 3. Global irradianations on a slope plane at 10° angle and on the wall (Kemajou *et al.* 2012).

Solar dryer design

The fan is the type SK012/4EHBWC. The electrical characteristics are 0,37kW power, 1350tr/min rate of rotation, 3,6A intensity, 240V tension and 50Hz frequency. The dryer dimensions are 3,10m length 2,40m width and 2,75m west height. The roof at the slope of 10 degrees with horizontal. The floor is well insulated to reduce the heat losses. Black body situated at the top of the dryer is made in a steel sheet (aluminum) with an inclination 10 degrees with horizontal, smooth $5^\circ/10^\circ$. Another physical parameters of the steel sheet are 0,5mm thickness, 2m length, 1m width and 2,7kg mass. The air volume in the dryer is equal to the dryer volume with the reduction of the volume of all other component located in the dryer. The obtained air volume is equal to 13m^3 . Layout of the dryer is presented in Figure 4.

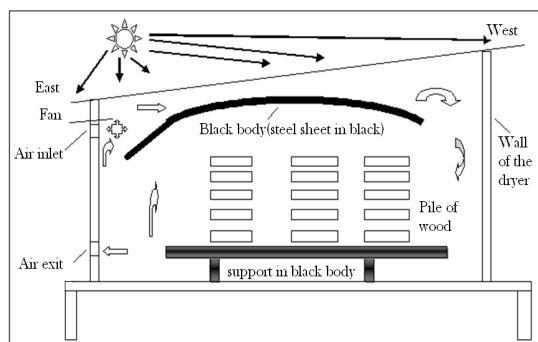


Figure 4. Schematic representation of the indirect solar dryer.

The wall and the slope are made in polyethylene. We have 3,7kg and $5,28\text{m}^2$ respectively the mass and surface of the east side wall. 4,623kg and $6,6\text{m}^2$ are respectively the mass and surface

of the west side wall. The north and south sides have the mass and surface respectively equal to 5,374kg and 7,673m². The mass and surface of the slope are 5,292kg and 7,555m² respectively.

Wood stack characteristics

We have 14 layers with 4 boards by layer. Two consecutive layers are separated by the sticks and each stick dimensions are 220cm length and 3,5cm thickness. Each board in the wood stack has 5cm thickness, 220cm length and 38,5cm width. Thus, the wood stack porosity is equal to 0,412. The total board surface and the total wood stack volume are respectively equal to 97,16m² and 2,156m³. Using the wood stack characteristics and the dryer dimensions, we obtained a fill factor (FF) equal to 0,195.

Modeling of the Dryer

Hypotheses taken are:

- *Each component inside the dryer is homogeneous;
- *The thermophysical characteristics of the air are only influenced by the temperature. The thermophysical characteristics of the black body and the wall are constant;
- *The entire wall has the same global solar radiation;
- *We neglected the variation between the days of the global solar radiation;
- *Natural convection is neglected;
- *The floor of the dryer is supposed adiabatic;
- *Transfers by conduction are neglected on all components of the dryer.

Model equations

Mass transfer on the wood stack:

We have used a purely diffusive mass transfer model such as Ananías *et al.* (2009, 2011), Bekkioui (2009), Bekkioui *et al.* (2009, 2011) and Bentayeb *et al.* (2008a, 2008b):

$$-m_0 \frac{dx}{dt} = KS_b(X - X_{eq}) \quad (4)$$

With: $m_0 = \rho_0(1 - \varepsilon)V_p = 1108,26 \text{ Kg}$ and $S_b = 2LpN_c(IN_{pc} + e_t) = 97,16m^2$. We have used $\rho_0 = 514,1 \text{ Kg} / m^3$ (Gérard *et al.* 1998).

Applied on temperate and Chilean woods, the literature proposes the variation of the global mass transfer coefficient K in function of the air temperature, air velocity, air relative humidity, fiber saturation point and equilibrium water content given on Equation (5) (Alvear *et al.* 2003, Ananías *et al.* 2009, Ananías *et al.* 2011, Bekkioui 2009, Bekkioui *et al.* 2009, Bekkioui *et al.* 2011, Bentayeb *et al.* 2008a, Bentayeb *et al.* 2008b):

$$\frac{1}{K} = a_0 \exp\left(\frac{C_0}{T_a}\right) e + b_0 \exp\left(\frac{C_0}{T_a}\right) V_{\text{int}}^{-p} \exp\left(-\frac{1-HR}{X_{fsp} - X_{eq}}\right) \quad (5)$$

$$a_0=0,2265\text{ms/kg}; b_0=268,9\text{m}^2/\text{kg}; c_0=2543,6\text{K}; p=2,7158$$

In this relation, e is used expressed in mm (Chrusciel *et al.* 1999). Simo-Tagne *et al.* (2016) show that it is possible to use the same influences of the global mass transfer coefficient in the case of tropical woods.

To estimate the external air temperature, we have used the relation (Benlahmidi 2013):

$$T_{aext} = \frac{T_{amin} + T_{amax}}{2} + \frac{T_{amax} - T_{amin}}{2} \text{Cos}\left(\pi \frac{t-12}{12}\right) \quad (6)$$

We have $T_{amax} = 303,75\text{K}$ and $T_{amin} = 292,95\text{K}$. Initially, we have taken the temperature of all the component of the dryer equal to the value $\frac{T_{amin} + T_{amax}}{2}$.

Mass transfer of air

The global mass balance of water in the dryer is given by Eq(7) taken from Bekkioui (2009), Bekkioui *et al.* (2009, 2011) and Bentayeb *et al.* (2008a, 2008b).

$$G(Y_s - Y_E) + m_a \frac{dY_s}{dt} + \rho_0(1 - \varepsilon)V_p \frac{dX}{dt} = 0 \quad (7)$$

With

$$m_a = \rho_a (V_{dryer} - (1 - \varepsilon)V_p) \quad (8)$$

$$G=0,05\text{kg/s.}$$

Air relative humidity (HR,-) is given by:

$$HR = \frac{P_{atm} Y_s}{P_{vsat} 0,622 + Y_s} \quad (9a)$$

$$P_{atm} = 101325 - 12z + 5,2 \times 10^{-4} z^2 \quad (\text{Galilée 2005}) \quad (9b)$$

with $z=720\text{m}$ for Yaoundé (Afungchui and Neban-Ngwa 2013).

$$P_{vsat} = 1,013125 \times 10^5 \exp\left(13,7 - \frac{5120}{T_a}\right), (\text{Nadeau and Puiggali 1995}) \quad (9c)$$

Thermal transfer on the wood stack

We have neglected the exchange between the wood stack and the floor, also between the wood stack and the cover. Thus the rate of accumulation of thermal energy in the product is equal to the sum of the rate of thermal energy gain from the product due to sensible and latent heat, the rate of thermal energy received from air by the product due to convection and the rate of radiation between black body and wood stack. Thus we have:

$$m_0 C_{pb} \frac{dT_b}{dt} = -K(L + E_b) S_b (X - X_{eq}) + h_b S_b (T_a - T_b) + \sigma S_{bb} F_{bb-b} (T_{to}^4 - T_b^4) \quad (10)$$

Thermal transfer of the air

The rate of accumulation of thermal energy in the air inside the dryer is written as the sum of the rate of solar energy accumulated inside dryer from solar radiation through the roof and the wall respectively, the rate of thermal energy change in the air chamber due to inflow and outflow of the air in the chamber, the rate of thermal energy loss from air inside due to latent heat, the rates of thermal energy exchanged by convection between inside air and the roof, between inside air and the wall, between inside air and the black body and between inside air and wood stack respectively. Thus we have:

$$m_a C_{pa} \frac{dT_a}{dt} = (1 - \alpha_p) S_p G_t^*(10^\circ) + (1 - \alpha_{pl}) S_{pl} G_t^*(\text{Wall}) + GC_{pa} (T_{aext} - T_a) + GL(Y_E - Y_S) - h_{cl} S_p (T_a - T_p) - h_{cil} S_{pl} (T_a - T_{pl}) - h_{cto} S_{to} (T_a - T_{to}) - h_{cb} S_b (T_a - T_b) \quad (11)$$

Thermal transfer on the black body

The rate of accumulation of thermal energy in the black body situated on the top of the drying chamber is equal to the sum of the rate of solar energy transferred by the roof and accumulated on the black body from solar radiation, the rate of thermal energy transfer by convection between the inside air and the black body, the rates of thermal energy exchanged by radiation between the roof and the black body, between the black body and the wall and between the black body and the wood stack respectively. Thus we have:

$$m_{to} C_{pto} \frac{dT_{to}}{dt} = \tau_p \alpha_{to} S_{to} G_t^*(10^\circ) - h_{to} S_{to} (T_{to} - T_a) - \sigma S_{to} F_{to-p} (T_{to}^4 - T_p^4) - \sigma S_{pl} F_{pl-to} (T_{to}^4 - T_{pl}^4) - \sigma S_{to} F_{to-b} (T_{to}^4 - T_b^4) \quad (12)$$

Thermal transfer of the roof slope in polyethylene

The rate of accumulation of thermal energy in the roof is equal to the sum of the rate of solar energy accumulated in the roof from solar radiation, the rate of thermal energy exchanged by radiation between the roof and the black body, and between the roof and the sky, the rate of thermal energy transferred by convection between the inside air and the roof, also between the outside air and the roof. Thus we have:

$$m_p C_{pp} \frac{dT_p}{dt} = \alpha_p S_p G_t^*(10^\circ) + \sigma S_p F_{p-to} (T_{to}^4 - T_p^4) + \sigma S_p F_{p-ciel} (T_{ciel}^4 - T_p^4) - \frac{1}{2} S_p h_{vint} (T_p - T_a) - \frac{1}{2} S_p h_{vext} (T_p - T_{aext}) \quad (13)$$

Thermal transfer on the wall of the dryer

The rate of accumulation of thermal energy in the wall (polyethylene cover) is equal to the sum of the rate of solar energy accumulated in the wall from solar radiation, the rate of thermal energy transfer by convection between the inside air and the wall, also between the outside air and the wall, the rate of thermal energy exchanged by radiation between the wall and the black body, and between the wall and the sky. Thus we have:

$$m_{pl} C_{ppl} \frac{dT_{pl}}{dt} = \alpha_{pl} S_{pl} G_t^* (Wall) - \frac{1}{2} S_{pl} h_{cint} (T_{pl} - T_a) - \frac{1}{2} S_{pl} h_{cext} (T_{pl} - T_{aext}) + \sigma S_{pl} F_{pl-to} (T_{to}^4 - T_{pl}^4) + \sigma S_{pl} F_{pl-ciel} (T_{ciel}^4 - T_{pl}^4) \quad (14)$$

The relations below are used in the program. Form factors are obtained after calculations with the dimensions of the components of the dryer.

$$T_{ciel} = 0,0552 T_{aext}^{1,5} \quad (15)$$

$$h_{cext} = 5,67 + 3,86 V_{ext} \quad (16)$$

$V_{ext} = 1,3 \text{ m/s}$ (meteorological data), $V_{int} = 1,5 \text{ m/s}$; $h_{cil} = 7 \text{ w}/(\text{m}^2\text{K})$; $h_{ci} = 8 \text{ w}/(\text{m}^2\text{K})$; $h_{cto} = 8 \text{ w}/(\text{m}^2\text{K})$;

$$h_b = \frac{N_u \lambda_{air}}{D_h}; N_u = 0,023 R_e^{0,8} P_r^{0,33}; R_e = \frac{V_{int} D_h}{u_{air}}; D_h = 2e_t \quad (17a)$$

We have $Re = 5687,36$; $D_h = 0,07 \text{ m}$; $Pr = 0,708$; $\lambda_{air} = 0,026248 \text{ w}/(\text{mK})$; $h_{cb} = 8 \text{ w}/(\text{m}^2\text{K})$. Thus we have $h_b = 7,77 \text{ w}/(\text{m}^2\text{K})$.

The thermophysical correlations on the wood and on the component of the dryer are taken in the literature Simo-Tagne (2014) and Simpson and TenWolde (1999). Those of air, black body (in aluminum) and wall (in polyethylene) are taken in the literature (Jannot 2011, Lienhard IV and Lienhard V 2011, Nadeau and Puiggali 1995). We have:

$$C_{pto} = 900 \text{ J}/(\text{kg}\cdot\text{K}); C_{pp} = C_{ppL} = 2300 \text{ J}/(\text{kg}\cdot\text{K}); \alpha_p = \alpha_{pL} = 0,05; \alpha_{to} = 0,91; \tau_p = 0,95;$$

$$C_{pa} = 1835 - 0,734(T_a - 273,15) \quad (17b)$$

$$L = 1000(3335 - 2,91T_a) \quad (17c)$$

$$E_b = 1170,4 \times 10^3 \exp(-14X) \quad (17d)$$

$$C_{pb} = \frac{C_{po} + XC_{pw}}{1+X} + X(-6,191 \times 10^{-4} + 2,36 \times 10^{-6} T_b - 1,33 \times 10^{-8} X) \quad (17e)$$

$$C_{po} = 0,1031 + 3,867 \times 10^{-3} T_b; C_{pw} = 4190 \text{ J}/(\text{Kg}\cdot\text{K}) \quad (17f)$$

Second term of second member of (17e) is equal to zero in a non-hygroscopic domain, domain that is limited by the water content at the fiber saturation points. The geometric factor is obtained using the method developed in Clark and Korybalsky (1974). This method is also used by Bekkioui (2009), Bekkioui *et al.* (2009, 2011) and Bentayeb *et al.* (2008). We have obtained:

$$F_{top}=0,537; F_{pciel}=0,8; F_{pto}=0,81; F_{pLto}=0,75; F_{tob}=0,3; F_{bbb}=0,323.$$

The parameter used to compare experimental and numerical results is given by the average relative error:

$$E_r (\%) = \frac{100}{N} \sum_{i=1}^N \frac{|X_{th_i} - X_{exp_i}|}{\frac{X_{th_i} + X_{exp_i}}{2}} \quad (18)$$

Method of Resolution and Experimental Drying Process

Method of resolution

Finite difference method (Gonçalves 2005) is used to resolve equation relative to the mass transfer on the air (Eq. 7). We obtained:

$$Y_{s,t1} = \frac{Y_{s,to} m_a + m_o (X_{to} - X_{t1}) + G Y_{E,t1} \Delta t}{m_a + G \Delta t} \quad (19)$$

Known air humidity of the air at the time t_0 , ($Y_{s,to}$) we deduced the air humidity at the time

$t_1 = t_0 + \Delta t (Y_{s,t1})$. For all the others relations, we have used Runge Kutta method in the order 4 (Gonçalves 2005). For example, Eq.10 is treated such as the following:

$$A(t_n, T_{bn}) = -K(L + E_b) S_b (X - X_{eq}) + h_b S_b (T_a - T_b) + \sigma S_{bb} F_{bb-b} (T_{to}^4 - T_b^4) \quad (20a)$$

$$f(t_n, T_{bn}) = \frac{A(t_n, T_{bn})}{m_o C_{pb}} \quad (20b)$$

Given T_{bo} we have:

$$k_1 = \Delta t f(t_n, T_{bn}) \quad (20c)$$

$$k_2 = \Delta t f\left(t_n + \frac{\Delta t}{2}, T_{bn} + \frac{k_1}{2}\right) \quad (20d)$$

$$k_3 = \Delta t f\left(t_n + \frac{\Delta t}{2}, T_{bn} + \frac{k_2}{2}\right) \quad (20e)$$

$$k_4 = \Delta t f(t_n + \Delta t, T_{bn} + k_3) \quad (20f)$$

$$T_{b_{n+1}} = T_{bn} + \frac{1}{6} (k_1 + 2k_2 + 2k_3 + k_4) \quad (20g)$$

Fortran language in the version 77 was used to generate our results and the step time used was 15s. We recorded our results each 1hr drying time.

Experimental drying process

The mission of promoting local materials of Cameroon (MIPROMALO) had built and experienced the solar dryer studied in this paper. After having positioned the wood stack, the fan is commanded ON. The air relative humidity inside is controlled after each two hours during the day. If the air relative humidity is more greater than 0,7 (near 0,9), the air inside is replaced by fresh outside air. When the air relative humidity inside is lower than 0,7 (near 0,3), the fresh air replaces the air inside the dryer. At night, inside air is exchanged each 1hr in order to avoid atmospheric saturation.

RESULTS AND DISCUSSION

Known that initial drying time 0 corresponds to 00pm (local time in Yaoundé). Figure 5 shows a satisfactory agreement between theoretical and experimental measurements. We have a average relative error E_r equal to 4,49%. From initial water content equal to 0,4kg/kg with the thickness equal to 50mm, 20days are necessary to dry iroko wood to 0,15kg/kg, Figure 5.

Figure 6 shows the influence of the environment on the water content of our wood. During the night, equilibrium water content is great and it is weak at 12 o'clock. Then, the drying of wood stack is weak during the night. It is clear that in this condition, the wood stack dried until the equilibrium value of 0,11kg/kg after 768h drying time, Figure 6.

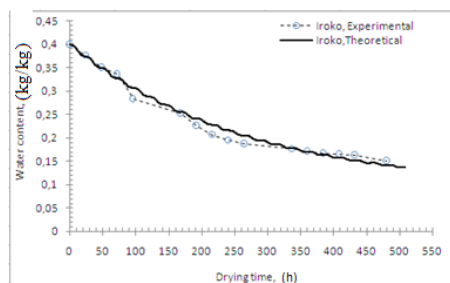


Figure 5. Experimental and theoretical water content evolution versus drying time, 50mm.

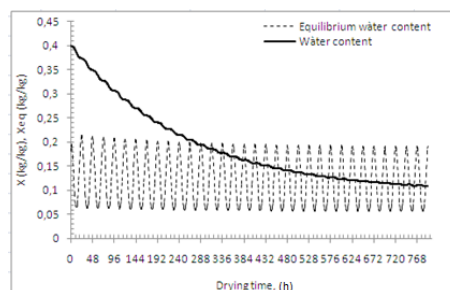


Figure 6. Theoretical water content and equilibrium water content evolutions versus drying time,

50mm.

If we want to use this solar dryer to dry our wood in order to use in a house in Yaoundé, knowing that the means values in the Yaoundé house are $HR=0,727$ and $T=24,8^{\circ}C$ (Kameni *et al.* 2014), relation (1a) gives equilibrium water content equal to $0,144kg/kg$ for our wood. In the same experimental process and climatic conditions, our indirect solar dryer gives these equilibrium values after 18days. Figure 7 shows the time variations of temperatures relative to the wood stack (red), to the interior air (blue) and to the black body (green) during 528hrs drying time. Curves are presented 528hrs of the drying process. We notice that the curves are similar evolutions than the temperature of the air outside the dryer. Black body absorbs most energy necessary to facilitate drying process during the night. Figure 8 shows that air relative humidity vary with the time. When air temperature increases, air relative humidity decreases. Also, air temperature inside the dryer is greater than air exterior with a difference equal to $10^{\circ}C$.

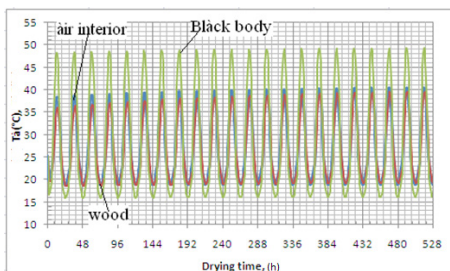


Figure 7. Predicted temperatures of wood stack, black body and air interior during the process, 50mm.

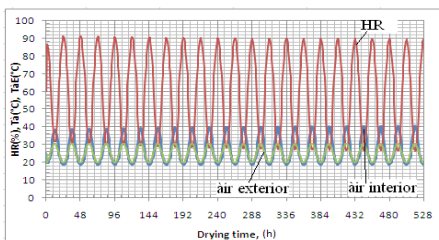


Figure 8. Theoretical relative humidity, outside air temperature and inside air temperature, 50mm.

Figure 9 presents the variation of average water content of wood stack with the drying time in function to the wood thickness numerically obtained. When wood thickness decreases, drying process is rapid. When the thickness changes, final water content is near than equilibrium water content.

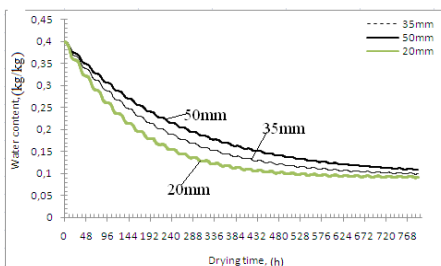


Figure 9. Predicted water content versus drying time and board thickness, 50mm.

Figure 10a shows that the drying kinetic is fast when initial water content is important because it is easy to dry free water. Also, final water content of all curves at different initial water content is near to equilibrium water content. It is clear that, if initial water content or thicknesses of wood are different, final water content of each plank is different. Thus, it is important to do a pretreatment to the wood stack in order to homogenize initial water content of the stack. Also, it is possible to do this homogenization at the end of the drying process with an increase of interior air relative humidity. Figure 10b shows that when air flow rate increases, drying kinetic decreases. Increase of air flow rate helps to decrease the value of air temperature because communication between air drying and the components of the dryer is reduced. Figure 11 presents the consequence of two types of ventilation of the dryer. Open night conduct (in the night, we remove moist air in the dryer) helps to increase drying kinetic, compared to the case where in the night fan is stopped. When moist air is not remove in the night, it is possible that interior air humidity becomes more than the board humidity at the surface. Thus, the drying kinetic becomes very lowest comparing by the case where ventilation is not stopped. It is clear that the drying duration is great in the case where ventilation is stopped during the night.

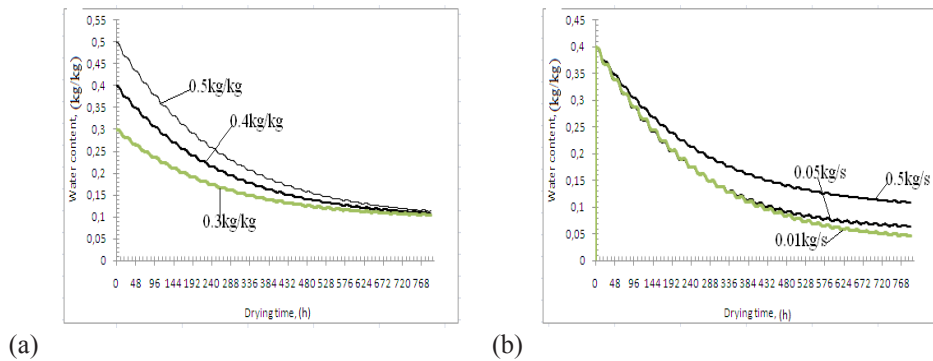


Figure 10. Predicted water content versus drying time with 50mm of thickness. (a) Influence of initial water content, (b) influence of air flow rate.

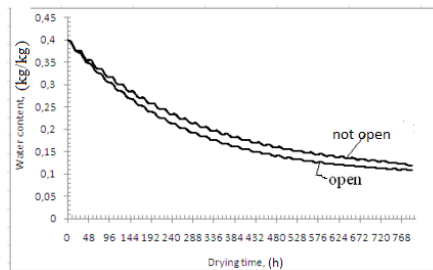


Figure 11. Predicted water content in function of the ventilation, 50mm.

CONCLUSIONS

The model developed gives a satisfactory agreement in comparison with experimental results. The influences of initial wood water content, airflow velocity and board thickness on the drying process are conformed. Mathematical model proposed can be used to design the performing dryer in order to build in tropical region many indirect solar dryers less expensive. During drying process, it is important to homogenize initial water content and the board thickness in order to obtain a same drying kinetic of each board. At night, it is economically important to stop the fan and open the drying chamber when inside air is near saturation. In the future, it will interesting to discuss which terms are important to carefully characterize in this model.

ACKNOWLEDGEMENTS

The principal author acknowledges the International Tropical Timber Organization (ITTO) for financially supporting a part of this work (ITTO Ref. Number: 012/15A). The authors are grateful to the administration and all staff of the mission of promoting local materials of Cameroon (MIPROMALO) for the experimental data given and all explanations obtained in order to put it in our program. We acknowledge the two anonymous reviewers for all suggestions given to ameliorate the presentation of this paper.

REFERENCES

- Afungchui, D.; Neba-Ngwa, R. 2013.** Global solar radiation of some regions of Cameroon using the linear Angstrom and non-linear polynomial relations (part I) model development. *International Journal of Renewable Energy Research* 3(4):984-992.
- Alvear, M.; Broche, W.; Salinas, C.; Ananias, R.A. 2003.** Drying kinetic of Chilean coigüe: Study of the global drying coefficient. *8th International IUFRO Wood Drying Conference*: 383-387.
- Ananías, R.A.; Chrusciel, L.; Zoulalian, A.; Salinas-Lira, C.; Mougel, E. 2011.** Overall mass transfer coefficient for wood drying curves predictions. *Mass Transfer in Multiphase Systems and its Applications*. [on line] Prof. Mohamed El-Amin (Ed.), ISBN: 978-953-307-215-9, InTech. Available from: <<http://www.intechopen.com/books/mass-transfer-in-multiphase-systems-and-its-applications/overall-masstransfer-coefficient-for-wood-drying-curves-predictions>>
- Ananías, R.A.; Mougel, E.; Zoulalian, A. 2009.** Introducing an overall mass-transfer coefficient for prediction of drying curves at low temperature drying rates. *Wood Science and Technology* 43(1):43-56.
- Awadalla, H.S.F.; El-Dib, A.F.; Mohamad, M.A.; Reuss, M.; Hussein, H.M.S. 2004.** Mathematical modelling and experimental verification of wood drying process. *Energy Conversion and Management* (45):197-207.
- Ayangma, F.; Nkeng, G.E. ; Bonoma, D.B.; Nganhou, J. 2008.** Evaluation du potentiel en énergie solaire au Cameroun : Cas du Nord Cameroun. *African Journal of Science and Technology, Science and Engineering series* 9(2):32-40.
- Bauer, K. 2003.** Development and optimization of a low temperature drying schedule for *Eucalyptus grandis* (Hill) ex maiden in a solar assisted timber dryer. Ph.D. Thesis, Institut für Agrartechnik in den Tropen und Subtropen, Universität Hohenheim, Germany.

- Bekkioui, N. 2009.** Séchage solaire du bois: modélisation simplifiée du séchage solaire d'une pile de bois dans un séchoir solaire à parois vitrées. Ph.D.Thesis, University of Mohammed V-AGDAL, Morocco.
- Bekkioui, N.; Hakam, A.; Zoulalian, A.; Sessbou, A.; Kortbi, M.E. 2011.** Solar drying of pin lumber: Verification of a mathematical model. *Maderas. Ciencia y Tecnología* 13(1):29-40.
- Bekkioui, N.; Zoulalian, A.; Hakam, A.; Bentayeb, F.; Sessbou, F. 2009.** Modelling of a solar wood dryer with glazed walls. *Maderas. Ciencia y Tecnología* 11(3): 191-205.
- Benlahmidi, S. 2013.** Etude du séchage convectif par l'énergie solaire des produits rouges. Ph.D.Thesis. University of Mohamed Khider-Biskra. Algeria.
- Bentayeb, F.; Bekkioui, N.; Camacho, E. F. 2008b.** Simulation of a solar dryer functioning in a Moroccan climate. *VI Minsk International Seminar. Heat Pipes, Heat Pumps, Refrigerators* : 214-219.
- Bentayeb, F.; Bekkioui, N.; Zeghmami, B. 2008a.** Modelling and simulation of a wood solar dryer in a Moroccan climate. *Renewable Energy* (33):501-506.
- Chrusciel, L.; Mougel, E.; Zoulalian, A.; Meunier, T. 1999.** Characterisation of water transfer in a low temperature convective wood drier: influence of the operating parameters on the mass transfer coefficient. *Holz Roh Werkstoff* (57):439-445.
- Clark, J.A.; Korybalski, M.E. 1974.** Algebraic methods for the calculation of radiation exchange in an enclosure. *Warme-und Stoffubertragung* 7:31-44.
- Galilée, L.P. 2005.** *L'air humide Cours de climatisation*, (Chapter 1). BTS Cours FEE 1^{ère} Année.
- Gérard, J.; Kouassi, A.E.; Daigremont, C.; Détienne, P.; Fouquet, D.; Vernay, M. 1998.** *Synthèse sur les caractéristiques technologiques de référence des principaux bois commerciaux africains*. Série FORAFRI, Document 11, CF, CIRAD, CIFOR.
- Gonçalves, E. 2005.** *Résolution numérique, discrétisation des EDP et EDO*. Institut National Polytechnique de Grenoble.
- Jannot, Y. 2011.** Thermique solaire. Cours de transfert thermique.
- Jannot, Y.; Kanmogne, A.; Talla, A.; Monkam, L. 2006.** Experimental determination and modelling of water desorption isotherms of tropical woods: afzelia, ebony, iroko, moabi and obeche. *Holz als Roh-und Werkstoff* (64):121-124.
- Kameni, N.M.; Tchinda, R.; Orosa, J.A.; Roshan, G. 2014.** Study of dioxide carbon concentration and indoor air quality in some buildings in the equatorial region of Cameroon (Yaoundé). *Iranian Journal of Health Sciences* 2(2):1-15.
- Kemajou, A.; Mba, L.; Pako-Mbou, G. 2012.** Energy efficiency in air-conditioned buildings of the tropical humid climate. *IJRRAS* 11(2):235-240.
- Lealea, T.; Tchinda, R. 2013.** Estimation of diffuse solar radiation in the South of Cameroon. *Journal of Energy Technologies and Policy* 3(6):32-42.
- Lienhard IV, J.H.; Lienhard V, J.H. 2011.** *A heat transfer textbook*. Fourth edition, Cambridge Massachusetts.
- Luna, D.L. 2008.** Modélisation et conception préliminaire d'un séchoir solaire pour bois de pin avec stockage d'énergie. Ph.D. Thesis, ENSAM, France.
- Luna, D.L.; Nadeau, J.P.; Jannot, Y. 2010.** Model and simulation of a solar kiln with energy storage. *Renewable Energy* 36(11):2533-2542.

Nadeau, J.P.; Puiggali, J.R. 1995. *Séchage, des processus physiques aux procédés industriels.* Paris, New York, Londres, Tec and Doc.

Njomo, D.; Wald, L. 2006. Solar irradiation retrieval in Cameroon from meteosat satellite imagery using Helio_2 method. *ISESCO Science and Technology Vision* 2(1):19-24.

Simo-Tagne, M. 2014. Numerical study of heat and mass transfer during the thermal drying of tropical woods. *International Journal of Thermal and Environment Engineering* 8(2):9-15.

Simo-Tagne, M.; Monkam, L.; Rémond, R.; Zoulalian, A.; Rogaume, Y.; Beguide-Bonoma. 2016. Experimental determination of the global mass transfer coefficient of the tropical woods in order to deduce the drying curves at the lower temperature. *International Journal of Thermal and Environment Engineering* 12(1):9-14.

Simpson, W.T.; TenWolde, A. 1999. *Physical properties and Moisture Relations of Wood.* Chapter 3 from Forest Products Laboratory. Wood handbook.

Weiss, W.; Buchinger, J. 2003. *Solar drying.* AEEE INTEC.

Appendix A

(Jannot 2011)

$S_t = G_t - D$; G_t , S_t and D are global, direct and diffuse insolation on horizontal plane.

For inclined plane i , we have: (A1)

$$G^*(i, \gamma) = S^*(i, \gamma) + D^*(i, \gamma) + R^*(i, \gamma)$$

$$S^*(i, \gamma) = \frac{S}{\sin(h)} [\cos(h) \sin(i) \cos(a - \gamma) + \sin(h) \cos(i)] \quad (A2)$$

$$D^*(i, \gamma) = \frac{D}{2} [1 + \cos(i)] \quad (A3)$$

$$R^*(i, \gamma) = \frac{G}{2} \rho [1 - \cos(i)] \quad (A4)$$

ρ is the albedo

h is height of the sun:

$$\sin(h) = \sin(\text{Lat}) \sin(\delta) + \cos(\text{Lat}) \cos(\delta) \cos(w) \quad (A5)$$

$$\sin(a) = \frac{\cos(\delta) \sin(w)}{\cos(h)} \quad (\text{A6})$$

a is azimuth; Lat is latitude; i is inclination angle; δ is declination; w is horar angle giving by

$$w = 15^\circ (\text{TS}-12) \quad (\text{A7})$$

TS is Solar time expressed in h.

$$\delta = 23,45^\circ \sin[0,98^\circ(j+284)] \quad (\text{A8})$$

j day number in the year ;

$$TS = TL - C + ET + \frac{l_{ref} - long}{15} \quad (\text{A9})$$

TL is the legal time (h), ET is Equation of the time (h) l_{ref} and $long$ are reference of longitude and longitude of the site ($^\circ$) respectively. We have used $C=1\text{h}$ and $l_{ref}=0^\circ$ for Yaoundé.

Nomenclature

C_{pa}	:	mass heat of the air (J/(kg.K));
C_{pto}	:	mass heat of the black body (J/(kg.K));
C_{pb}	:	mass heat of the wood (J/(kg.K));
C_{pp}	:	mass heat of the roof slope (polyethylene) (J/(kg.K));
C_{ppl}	:	mass heat of the wall (polyethylene) (J/(kg.K));
D	:	diffuse solar irradiation on a horizontal plane (w/m^2);
$\frac{d}{dt}$:	derivative with respect of the drying time (s^{-1});
e	:	thickness of the plank (mm);
E_b	:	desorption heat (J/kg);
E_r	:	average relative error (%);
e_t	:	stick thickness (m);
F_{bb-b}	:	geometric factor black body-wood(-);
FF	:	volume of the wood stack divided by the volume of the dryer chamber (-);

$F_{pl-ciel}$:	geometric factor between wall and sky (-);
F_{pl-to}	:	geometric factor between wall and black body (-);
F_{p-ciel}	:	geometric factor between roof slope and sky (-);
F_{to-b}	:	geometric factor between black body and wood (-);
G	:	mass flow rate of dry air (kg/s);
G_t	:	global solar radiation on a horizontal plane (w/m^2),
$G_t^*(10^\circ)$:	global solar radiation on the roof (w/m^2);
$G_t^*(Wall)$:	global solar radiation on the wall (w/m^2);
h_b	:	convective transfer between wood and air ($w/(m^2K)$);
h_{cb}	:	interior convective coefficient between the wood stack and the air ($w/(m^2K)$);
h_{cext}	:	convective coefficient between exterior air and wall ($w/(m^2K)$);
h_{ci}	:	interior convective coefficient between the roof slope and the air ($w/(m^2K)$);
h_{cil}	:	interior convective coefficient between the wall and the air ($w/(m^2K)$);
h_{cto}	:	interior convective coefficient between the black body and the air ($w/(m^2K)$);
HR	:	air relative humidity (-);
h_{vext}	:	convective coefficient between exterior air and the roof slope ($w/(m^2K)$);
h_{vint}	:	convective coefficient between interior air and the roof slope ($w/(m^2K)$);
K	:	mass global transfer coefficient ($kg/(m^2s)$);
l	:	width of each plank (m);
L	:	latent heat of evaporation (J/kg);
L_p	:	length of each plank (m);
Pr	:	Prandtl number (-);
P_{vsat}	:	pressure of vapor in saturation (Pa);
R	:	perfect gas constant ($8.314J/(mol.K)$);
r	:	regression of determination (-);
S_b	:	total exchange surface of the wood (m^2);
S_{bb}	:	black body surface (m^2);
S_p	:	surface of the roof slope (m^2);
S_{pl}	:	surface of the wall (m^2);
t	:	drying time (s);
T_a	:	interior air temperature (K);
T_{aext}	:	temperature of the air exterior of the dryer (K);
T_{amax}	:	maximum air temperature (K);
T_{amin}	:	minimum air temperature (K);
T_b	:	wood temperature (K);
T_{ciel}	:	temperature of the sky (K);
T_{pl}	:	temperature of the wall (K);
T_{to}	:	black body temperature (K);
V_{ext}	:	ambient air velocity (m/s);
V_{int}	:	air velocity inside dryer(m/s);
V_{dryer}	:	volume of the dryer (m^3);
V_p	:	wood stack volume (m^3);
X	:	water content of the wood stack in dry basis (kg/kg);
X_{eq}	:	equilibrium water content in dry basis (kg/kg);
X_{fsp}	:	fractional moisture content in dry basis at the fiber saturation point(kg/kg);
X_m	:	fractional moisture content in dry basis at the monolayer saturation point (kg/kg);

$X_{exp,i}$:	experimental water content of the wood stack in dry basic number i (kg/kg);
$X_{th,i}$:	theoretical water content of the wood stack in dry basic number i (kg/kg);
Y_E	:	inlet air humidity of the dryer (kg/kg);
Y_S	:	inside air humidity of the dryer (kg/kg);
z	:	altitude of the dryer (the one of the town)(m);
α_p	:	absorptivity of the roof (-);
α_{pL}	:	absorptivity of the wall (-);
α_{to}	:	absorptivity of the black body (-);
τ_p	:	transmittivity of the roof and wall (-);
λ_{air}^p	:	thermal conductivity of the air(W/(m.K));
μ_{air}	:	dynamical viscosity of the air(Pa.s);
ε	:	wood stack porosity (-);
ρ_a	:	air density (kg/m ³);
ρ_o	:	wood dry density (kg/m ³);
σ	:	Stefan-Boltzmann constant value (5,67x10 ⁻⁸ W / (m ² K ⁴);
Δt	:	time step (s);
$ $:	symbol of the absolute value.